

Note

Orientated growth of crystalline anhydrous maltitol
(4-*O*- α -D-glucopyranosyl-D-glucitol)F. Capet,^{a,*} S. Comini,^b G. Odou,^a P. Looten^b and M. Descamps^a^a*Laboratoire de Dynamique et Structure des Matériaux Moléculaires, U.M.R. CNRS n°8024, Université de Lille I,
F-59655 Villeneuve d'Ascq, France*^b*Roquette Frères SA, F-62136 Lestrem, France*

Received 6 August 2003; received in revised form 6 January 2004; accepted 16 February 2004

Abstract—In the industrial crystallisation process of maltitol ($C_{12}H_{24}O_{11}$), the presence of maltotriitol ($C_{18}H_{34}O_{16}$) in the maltose syrup is responsible for a change of the crystal morphology. Two different crystal forms of maltitol were obtained: a prismatic one and a 'bipyramidal' one.

IR and X-ray diffraction experiments (single crystal and powder) were performed to identify both crystal parameters. It is concluded that a structural polymorphism has to be ruled out. Close coincidences in some of the crystal cell parameters of maltitol and maltotriitol allow to assume the process through which maltotriitol affects the morphology of maltitol crystals.

© 2004 Elsevier Ltd. All rights reserved.

Keywords: X-ray structure; Oriental growth; Crystal habit; Alditols; Maltitol

Maltitol (4-*O*- α -D-glucopyranosyl-D-glucitol) is obtained by catalytic hydrogenation of maltose syrups. Because of its sweetness and relatively low energetic value, maltitol is widely used as a sweetener in low-calorie diet. It is also a compound of very high thermal and chemical stability.

Maltitol has been known for many years as an amorphous hygroscopic solid. The crystal structure of anhydrous maltitol was first reported in 1982.¹ A second report followed in 1989.² The hydrogen-bonding scheme has been proposed based on a redetermination of the crystal structure.³ These three successive investigations have led to the crystal structure of anhydrous maltitol as given by the orthorhombic space group $P2_12_12_1$, $Z = 4$. Reported values for the cell parameters are given in Table 1.

It has been observed recently,⁴ in the course of industrial crystallisation of maltitol, that residual maltotriitol (α -D-glucopyranosyl-(1 \rightarrow 4)- α -D-glucopyranosyl-(1 \rightarrow 4)-D-glucitol) in the syrup is responsible for

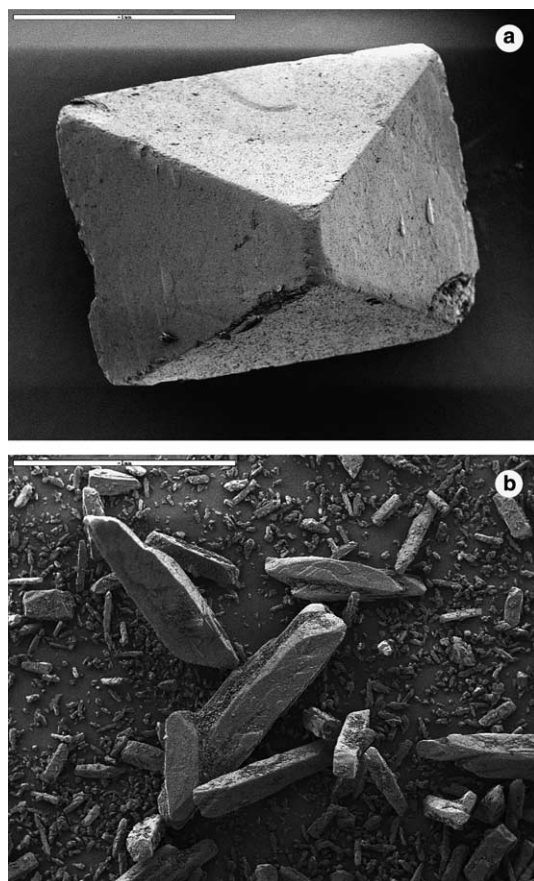
a change of the crystal morphology of maltitol. A 'bipyramidal' form is obtained when the ratio maltotriitol/maltitol is less than 1%, whereas the more elongated 'prismatic' form is obtained with a ratio greater than 4% (Fig. 1). Such a typical effect of an 'additive' on the modification of a crystal form has been reported for sucrose.⁵ In this case, a modification of the crystal form is observed depending on the presence of raffinose.

The two forms of maltitol may present some advantages or disadvantages both for manufacture and for applications. For example, partially crystallised maltitol shows differences in viscosity depending on whether it contains 'prismatic' or 'bipyramidal' crystals. Therefore, suspensions with 'bipyramidal' crystals would be preferred to prepare atomised maltitol, so as to avoid caking. In other respects, the use of 'bipyramidal' maltitol showed several interesting advantages in formulation, that is: (i) a more thickened mass before refining in the production of chocolate; (ii) a possibility of retaining a flexible texture with a large amount of powdered maltitol in the production of chewing-gums; (iii) a greater consistency of flow in the production of pharmaceutical dry forms.

* Corresponding author. Tel.: +33-320-43-6947; fax: +33-320-43-6847;
e-mail: frederic.capet@univ.lille1.fr

Table 1. Cell parameters for anhydrous maltitol crystals

Cell parameters (Å)	From Ref. 1	From Ref. 2	From Ref. 3
<i>a</i>	8.166(5)	8.170(1)	8.1269(5)
<i>b</i>	12.721(9)	12.731(1)	12.6888(8)
<i>c</i>	13.629(6)	13.679(3)	13.6581(5)

**Figure 1.** Scanning electron microphotography of anhydrous maltitol crystals: (a) 'bipyramidal', (b) 'prismatic'.

On the other hand, a 'prismatic' form is more compressible and enables low crystal content caking, as it is sometimes required for the production of chewing-gum to be sugar coated, as an example.

The aim of the present study is to describe these two maltitol crystal morphologies and to analyse their structural basis. The first specific purpose of these investigations was to determine if the two crystal forms could correspond to different polymorphic varieties of maltitol. Preliminary powder X-ray investigations as described below suggest this possibility. Therefore, powder and single crystal X-ray diffraction techniques were used to check the crystal structures of the two types of crystals and index the crystal faces of the two morphologies with regard to crystal unit cells. This work enables us to localise the preferred molecular orientations with regard to the most prominent faces.

Finally, a comparison of the structures of maltitol and maltotriitol in relation to the two crystal forms suggests that maltotriitol could behave as a crystallisation modifier of maltitol.

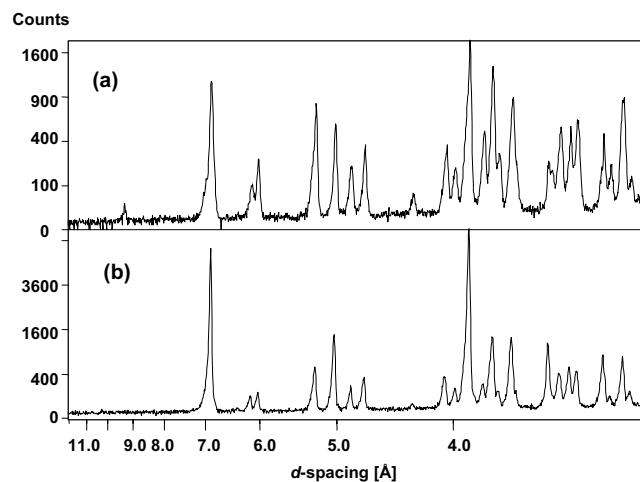
1. Maltitol crystal structure

Preliminary powder X-ray investigations on the two forms of maltitol were first performed using a flat sample spinner. The corresponding diagrams are presented in Figure 2. They look very similar despite some differences, among which (i) at small angles, the presence or not of a Bragg peak at d -spacing=9.3 Å; (ii) at intermediate angles, the lines are observed at the same positions but with large differences in relative intensity; at large angles (d -spacing < 4 Å), it is very difficult to resolve the spectra whose outlook is rather different.

In order to find the possible origin of these peculiar features, we carried out infrared and single-crystal X-ray experiments.

Infrared spectra (Fig. 3) of 'bipyramidal' and 'prismatic' maltitol crystals are identical to the one previously described for anhydrous crystalline maltitol,⁶ which seems to exclude a polymorphic difference.

By X-ray diffraction, single crystals of maltitol with the two different morphologies were analysed with the SMART diffractometer at room temperature. The dimensions of the crystals were 0.208*0.208*0.208 mm for the bipyramidal crystal and 0.480*0.112*0.112 mm for the prismatic one. The diffraction data were obtained by collecting 600 frames at each of three ϕ settings 0°, 120° and 240°, using a scan width of 0.3° in ω . The exposure time was 25 and 40 s per frame for the prismatic sample and the bipyramidal one, respectively.

**Figure 2.** Powder X-ray diffraction patterns (flat samples) of (a) 'bipyramidal', (b) 'prismatic' anhydrous maltitol crystals.

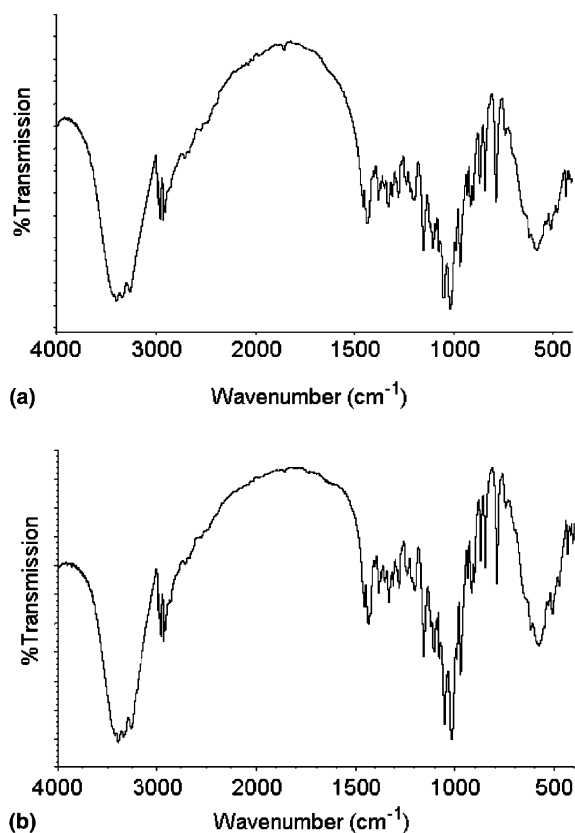


Figure 3. FT-IR spectrum of anhydrous maltitol crystals: (a) 'bipyramidal', (b) 'prismatic'.

The program Saint plus 6.02⁷ was used to extract the reflections from collected frames and to correct the corresponding intensities for Lorentz and polarisation effects. The unit cell parameters could then be refined using all reflections of the data set.

The study of systematic absences was performed using Bruker's xprep program of the shelxtl package⁸ and confirmed that both morphologies are associated to the orthorhombic space group $P2_12_12_1$. The crystal structures of both samples were solved by direct methods using the program SHELXS97.⁹ Refinements were carried out by full matrix least squares method with the SHELXL97 program;¹⁰ the threshold expression of $F > 4\sigma(F)$ was used only for calculating R -factors and is not relevant to the choice of reflections for refinement. The hydroxyl hydrogen atoms were located from difference Fourier maps and were included in the refinement. The non-hydroxyl hydrogen atoms were placed in theoretical positions and refined riding on their parent atoms. To each hydrogen atom was assigned an isotropic thermal parameter 1.2 times the equivalent isotropic U of the atoms to which it is attached (1.5 for the $-\text{OH}$). The most important details concerning crystal data, experiment and refinement are summarised in Table 2. Fractional positional parameters of the non-hydrogen atoms for the two forms are presented in

Table 3 together with those already reported.³ The equivalent thermal parameters U_{eq} for Ref. 3 are smaller than those of our studies because they were obtained at 95 and 298 K, respectively. All the results are similar to those previously reported. They demonstrate that the two samples have the same crystallographic structure parameters with two different morphologies. A representation of the maltitol molecule is shown in Figure 4.

In order to clarify the observed differences in the powder X-ray spectra of the two forms, we have performed a new investigation in transmission geometry using a capillary spinner (Inel CPS120 X-ray diffractometer). The diagrams (Fig. 5) are identical for both bipyramidal and prismatic forms. This proves that the differences revealed by preliminary X-ray experiments can be understood as resulting from preferred orientation of crystallites in the powder on the flat sample holder, which are not sufficiently averaged by the spinning motion.

2. Maltitol crystal morphology

The crystal unit cell and orientation matrix determinations were used to index the faces of the two samples. This was performed by determining edge-on positions of the faces as viewed through the goniometer telescope of the SMART diffractometer.

All the faces of the bipyramid could be identified as bounded by the low index forms: $(1\bar{1}0)$ $(\bar{1}10)$ (110) $(\bar{1}\bar{1}0)$ (011) $(0\bar{1}1)$ (011) $(0\bar{1}\bar{1})$.

The lateral faces of the prismatic crystal were identified to be: $(1\bar{1}0)$ $(\bar{1}10)$ (110) $(\bar{1}\bar{1}0)$. Unfortunately, the tip of the prismatic grown crystal was too thin for identifying the faces corresponding to the termination along the c -axis; they were approximated as (001) and $(00\bar{1})$ for representation convenience.

This reveals clearly the preferred growth mode of the prismatic crystal where the c -axis is the fast growing one. The growth rate of the faces, which lie in the zone of the c -axis are apparently slowed down owing to the presence of the maltotriitol additive in the syrup.

Images of the two forms with relative positions of the molecules are shown in Figures 6 and 7. The molecules are orientated approximately perpendicular to the a,c -plane and parallel to the b -axis.

The indexing of the faces may help the understanding of the preferred orientation effects revealed using the flat sample X-ray diffraction (Bragg–Brentano geometry). Actually, the most noticeable difference is observed at the level of the smallest angle (011) Bragg peak, which exists for the bipyramidal sample and totally disappears for the prismatic sample. It is worth noting that this peak is present with equal intensity in the more averaged capillary experiment. This seems correlated with the fact that (011) is a face of the bipyramid and not of the

Table 2. Crystal data, data collection and refinement parameters for anhydrous maltitol crystals

	Prismatic sample	Bipyramidal sample
<i>Crystal data</i>		
Formula	C ₁₂ H ₂₄ O ₁₁	C ₁₂ H ₂₄ O ₁₁
Molecular weight	344.32	344.32
Crystal size (mm)	0.48 × 0.11 × 0.11	0.21 × 0.21 × 0.21
Crystal colour	Colourless	Colourless
Crystal system	Orthorhombic	Orthorhombic
Space group	<i>P</i> 2 ₁ 2 ₁ 2 ₁	<i>P</i> 2 ₁ 2 ₁ 2 ₁
<i>Z</i>	4	4
<i>a</i> (Å)	8.152(1)	8.158(1)
<i>b</i> (Å)	12.705(2)	12.713(2)
<i>c</i> (Å)	13.640(2)	13.646(2)
<i>V</i> (Å ³)	1412.7(7)	1415.1(5)
<i>D_c</i> (g cm ⁻³)	1.6238(1)	1.6238(1)
<i>F</i> (000)	736	736
μ (cm ⁻¹)	1.4	1.4
λ (MoK α) (Å)	0.71073	0.71073
Temperature of study (K)	298	298
Crystal faces	(1 $\bar{1}$ 0) ($\bar{1}$ 1 0) (1 1 0) ($\bar{1}$ $\bar{1}$ 0)	(1 $\bar{1}$ 0) ($\bar{1}$ 1 0) (1 1 0) ($\bar{1}$ $\bar{1}$ 0) (0 1 $\bar{1}$) (0 $\bar{1}$ 1) (0 1 1) (0 $\bar{1}$ $\bar{1}$).
<i>Data collection</i>		
Instrument	Bruker smart CCD area detector diffractometer	Bruker smart CCD area detector diffractometer
Scan mode	0.3° ω -scan	0.3° ω -scan
Number of measured reflections	11,796	14,448
Number of independent reflections	3495	4201
Number of reflections with $F > 4\sigma(F)$	1754	2221
<i>R</i> _{int}	0.0715	0.0683
2 θ _{max}	57.80	61.84
Limiting <i>hkl</i>	−11 ≤ <i>h</i> ≤ 10	−11 ≤ <i>h</i> ≤ 11
	−17 ≤ <i>k</i> ≤ 17	−18 ≤ <i>k</i> ≤ 18
	−18 ≤ <i>l</i> ≤ 18	−19 ≤ <i>l</i> ≤ 19
<i>Refinement</i>		
Refinement method	Least square on <i>F</i> ²	Least square on <i>F</i> ²
<i>R</i> [<i>F</i> > 4 σ (<i>F</i>)]	0.0377	0.0348
<i>wR</i> (<i>F</i> ²)	0.0590	0.0607
Goodness of fit (<i>S</i>)	0.729	0.722
Number of refined parameters	235	235
Weighting scheme	$w = 1/[\sigma^2(F_o^2) + (0.0128P)^2]$ where $P = (F_o^2 + 2F_c^2)/3$	$w = 1/[\sigma^2(F_o^2) + (0.0176P)^2]$ where $P = (F_o^2 + 2F_c^2)/3$
(Δ/σ) _{max}	−0.001	0.001
$\Delta\rho$ _{max} (e Å ⁻³)	0.18	0.18
$\Delta\rho$ _{min} (e Å ⁻³)	−0.20	−0.15

prismatic sample, which lies preferentially on the flat rotating sample holder. On the other hand, similar intensities are found at the level of the (1 1 0) reflections, which correspond to faces equally developed for both morphologies.

In conclusion, detailed considerations in stereochemistry and interaction energy would certainly be necessary to account for the detail of morphology changes of maltitol crystals that are clearly identified in this work. We have however noticed close connections between several crystal lattice features of maltitol and maltotriitol. These connections may be of interest if we try to find structural features, which favour specific growth directions.

From the crystal structure determination of both compounds,^{3,11} it is remarkable that maltitol (ti) and

maltotriitol (tri) both crystallise in the *P*2₁2₁2₁ orthorhombic structure with almost the same *a*-parameter (*a*_{tri} = 8.1592 Å; *a*_{ti} = 8.1269 Å) and with the *c*_{tri} parameter of maltotriitol being quite exactly two times that of maltitol (*c*_{tri} = 27.8229 Å; *c*_{ti} = 13.6581 Å)—note that the temperature of study of the maltitol (95 K) was less than for maltotriitol (150 K). The *b*-parameters only are different (*b*_{tri} = 9.9951 Å; *b*_{ti} = 12.6888 Å). These relations are illustrated in Figure 8. From this, it appears that maltotriitol is certainly more capable to enter the growing surfaces of maltitol crystals where both crystals adapt their cell. One may think that a faster growth along the *c*-direction would be favoured by the possibility to stack rather indifferently maltitol and maltotriitol cells in this direction. On the contrary, the growth rate in a direction perpendicular to *c* and

Table 3. Reported fractional positional parameters of non-hydrogen atoms for anhydrous maltitol crystals: (1st line) ‘prismatic’, (2nd line) ‘bipyramidal’, (3rd line) results of Ref. 3

	<i>x</i>	<i>y</i>	<i>z</i>	<i>U</i> _{eq}
C-1	0.1421(3)	0.4776(2)	0.1110(2)	0.0226(6)
	0.1415(2)	0.4773(1)	1.1112(1)	0.0238(4)
	0.1412(2)	0.4777(1)	0.1110(1)	0.0099(4)
C-2	0.0948(3)	0.4039(2)	0.1950(2)	0.0231(6)
	0.0954(2)	0.4041(2)	1.1953(1)	0.0250(4)
	0.0942(2)	0.4031(1)	0.1951(1)	0.0108(4)
C-3	0.1740(3)	0.2960(2)	0.1856(2)	0.0227(6)
	0.1734(2)	0.2957(1)	1.1853(1)	0.0244(4)
	0.1738(2)	0.2946(1)	0.1851(1)	0.0107(4)
C-4	0.1584(3)	0.2532(2)	0.0823(2)	0.0238(6)
	0.1584(2)	0.2531(1)	1.0821(1)	0.0243(4)
	0.1593(2)	0.2518(1)	0.0808(1)	0.0105(4)
C-5	0.2185(3)	0.3339(2)	0.0090(2)	0.0222(6)
	0.2194(2)	0.3336(1)	1.0086(1)	0.0232(4)
	0.2211(2)	0.3338(1)	0.0079(1)	0.0104(4)
C-6	0.2067(3)	0.2993(2)	−0.0968(2)	0.0299(7)
	0.2068(2)	0.2995(2)	0.9032(1)	0.0303(5)
	0.2093(2)	0.2989(1)	−0.0980(1)	0.0130(5)
C-11	0.4073(3)	0.8831(2)	0.1653(2)	0.0317(7)
	0.4068(3)	0.8835(1)	1.1656(2)	0.0324(5)
	0.4082(2)	0.8850(1)	0.1666(1)	0.0127(4)
C-12	0.4446(3)	0.7905(2)	0.1000(2)	0.0233(6)
	0.4442(2)	0.7904(1)	1.1004(1)	0.0249(4)
	0.4468(2)	0.7917(1)	0.1010(1)	0.0109(4)
C-13	0.3419(3)	0.6962(2)	0.1309(2)	0.0213(6)
	0.3414(2)	0.6965(1)	1.1310(1)	0.0237(4)
	0.3413(2)	0.6975(1)	0.1314(1)	0.0099(4)
C-14	0.3612(3)	0.5973(2)	0.0689(2)	0.0200(6)
	0.3613(2)	0.5974(1)	1.0685(1)	0.0225(4)
	0.3621(2)	0.5976(1)	0.0688(1)	0.0095(4)
C-15	0.5350(3)	0.5725(2)	0.0341(2)	0.0223(6)
	0.5349(2)	0.5715(1)	1.0334(1)	0.0235(4)
	0.5366(2)	0.5726(1)	0.0332(1)	0.0103(4)
C-16	0.6447(3)	0.5218(2)	0.1097(2)	0.0262(6)
	0.6444(2)	0.5223(1)	1.1096(1)	0.0276(4)
	0.6472(2)	0.5217(1)	0.1096(1)	0.0115(4)
O-1	0.3048(2)	0.5077(1)	0.1254(1)	0.0231(4)
	0.3048(1)	0.5081(1)	1.1253(1)	0.0244(3)
	0.3057(1)	0.5081(1)	0.1253(1)	0.0102(3)
O-2	0.1312(2)	0.4510(2)	0.2870(1)	0.0347(5)
	0.1316(2)	0.4509(1)	1.2871(1)	0.0348(4)
	0.1317(2)	0.4502 (1)	0.2874(1)	0.0139(3)
O-3	0.0944(2)	0.2272(1)	0.2535(1)	0.0374(5)
	0.0950(2)	0.2273(1)	1.2537(1)	0.0372(4)
	0.0944(2)	0.2249(1)	0.2524(1)	0.0145(3)
O-4	0.2520(2)	0.1594(1)	0.0737(1)	0.0338(5)
	0.2527(2)	0.1592(1)	1.0737(1)	0.0337(4)
	0.2552(2)	0.1581(1)	0.0722(1)	0.0136(3)
O-5	0.1198(2)	0.4274(1)	0.0193(1)	0.0243(4)
	0.1196(2)	0.4272(1)	1.0193(1)	0.0251(3)
	0.1194(1)	0.4272(1)	0.0185(1)	0.0106(3)
O-6	0.0494(2)	0.2660(1)	−0.1258(1)	0.0358(5)
	0.0501(2)	0.2661(1)	0.8744(1)	0.0353(4)
	0.0499(1)	0.2656(1)	−0.1269(1)	0.0148(3)
O-11	0.5248(3)	0.9664(1)	0.1571(1)	0.0351(5)
	0.5245(2)	0.9667(1)	1.1571(1)	0.0329(4)
	0.5276(2)	0.9688(1)	0.1584(1)	0.0133(3)
O-12	0.4143(2)	0.8212(1)	0.0017(1)	0.0334(5)
	0.4140(2)	0.8214(1)	1.0017(1)	0.0340(4)
	0.4170(2)	0.8232(1)	0.0020(1)	0.0138(3)

(continued on next page)

Table 3 (continued)

	<i>x</i>	<i>y</i>	<i>z</i>	<i>U</i> _{eq}
O-13	0.1707(2)	0.7265(1)	0.1254(1)	0.0296(5)
	0.1707(2)	0.7265(1)	1.1253(1)	0.0310(4)
	0.1702(1)	0.7282(1)	0.1256(1)	0.0128(3)
O-15	0.5294(2)	0.4954(1)	−0.0437(1)	0.0301(5)
	0.5294(2)	0.4957(1)	0.9563(1)	0.0295(4)
	0.5309(1)	0.4961(1)	−0.0446(1)	0.0120(3)
O-16	0.6605(2)	0.5857(1)	0.1954(1)	0.0369(5)
	0.6605(2)	0.5856(1)	1.1954(1)	0.0363(4)
	0.6607(2)	0.5852(1)	0.1963(1)	0.0143(3)

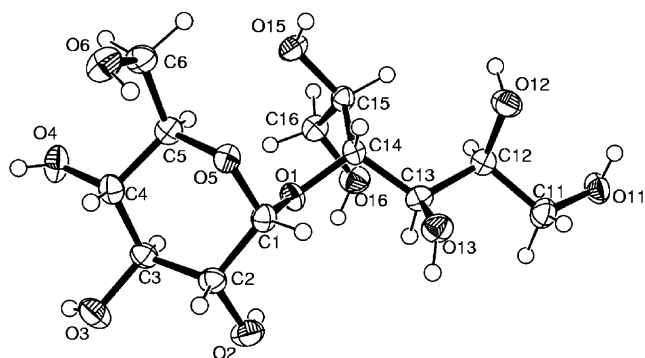


Figure 4. ORTEP representation of the molecule of maltitol.

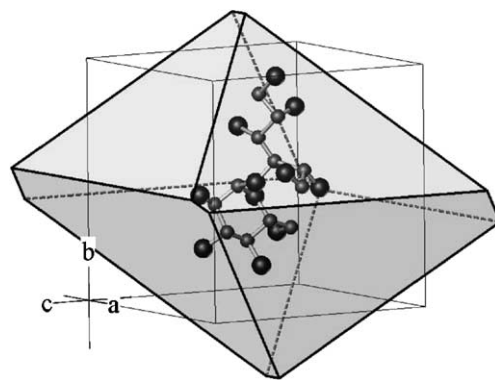


Figure 6. Maltitol in its 'bipyramidal' form (ATOMS V6.0 by Shape Software).

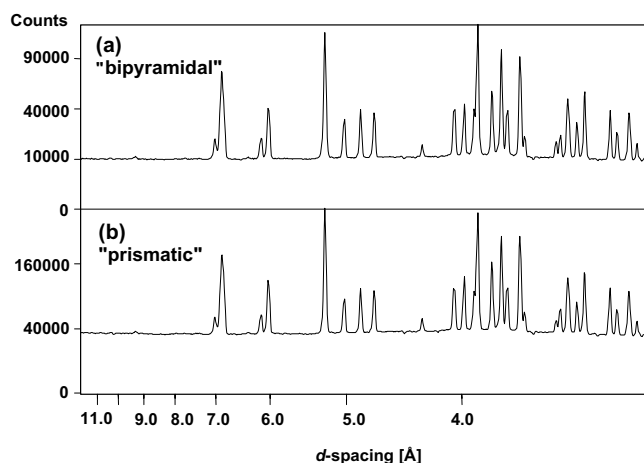


Figure 5. Powder X-ray diffraction patterns (capillary samples) of (a) 'bipyramidal', (b) 'prismatic' anhydrous maltitol crystals.

involving *b* is slowed down due to the need of removal of the strongly bonded maltotriitol impurity.

3. Experimental

Colourless 'bipyramidal' and 'prismatic' crystals of anhydrous maltitol (Fig. 1) were obtained according to the procedure in Ref. 4.

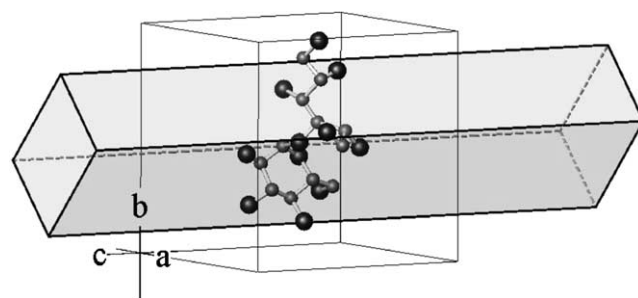


Figure 7. Maltitol in its 'prismatic' form (ATOMS V6.0 by Shape Software).

Infrared spectra were recorded on a Nexus (Nicolet) FT-IR spectrometer equipped with Omnic E.S.P. software, samples were analysed as KBr pellets.

Powder X-ray diffraction patterns were recorded on an X'Pert-MPD system (Philips) equipped with a Co X-ray tube and a PW1774/90 flat sample spinner, and on a Inel CPS120 equipped with a Cu X-ray tube, a curved quartz monochromator and a capillary spinner. Samples were moderately milled before the analysis.

Single crystal X-ray diffraction data were collected on a SMART 1K CCD (Bruker AXS) automatic diffractometer. This instrument uses graphite monochroma-

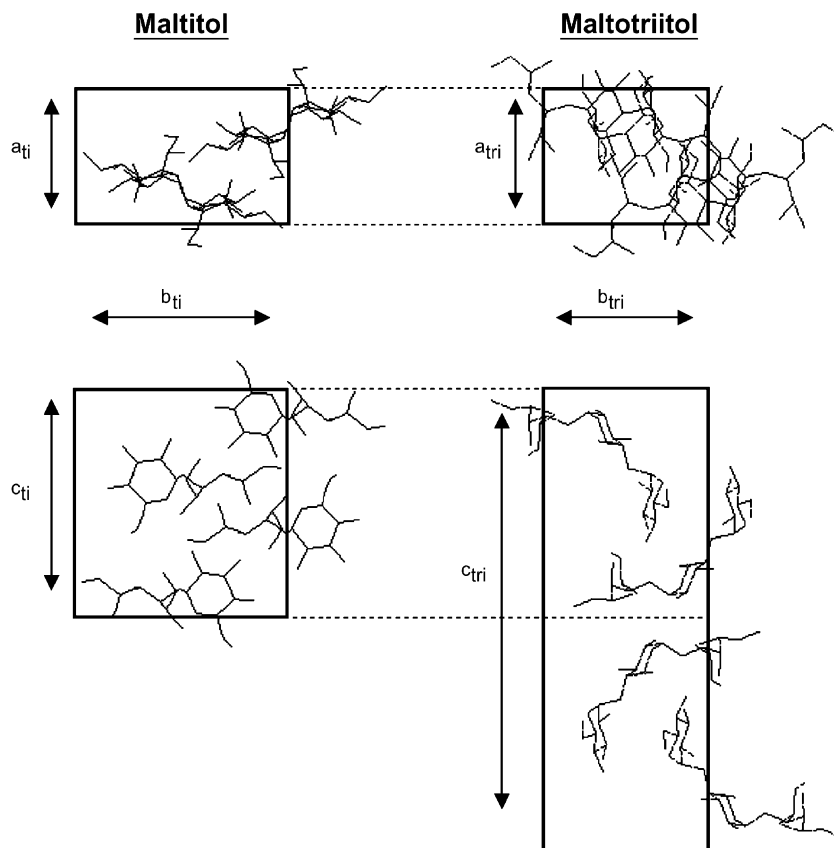


Figure 8. Comparison of cells of maltitol and maltotriitol.

tised MoK α radiation ($\lambda = 0.71073 \text{ \AA}$) and was operating at 50 kV \times 40 mA.

References and notes

1. Ohno, S.; Hirao, M. *Carbohydr. Res.* **1982**, *108*, 163–171.
2. Ja Park, Y.; Mi Shin, J.; Shin, W.; Suh, Il.-H. *Bull. Korean Chem. Soc.* **1989**, *10*, 352–356.
3. Schouten, A.; Kanters, J. A.; Kroon, J.; Looten, P.; Duflot, P.; Mathlouthi, M. *Carbohydr. Res.* **1999**, *322*, 298–302.
4. Leleu, J. B.; Haon, P.; Duflot, P.; Looten, P. U.S. Patent 6,344,591, 2002; *Chem. Abstr.* **1999**, *130*, 223540e.
5. Mantovani, G. *Rev. 3rd Int. Symp. AVH Assoc.*, Reims, March 1996, 19–29.
6. Hirao, M.; Hijiya, H.; Miyahe, T. Fr. Patent 2,499,576, 1982; *Chem. Abstr.* **1982**, *97*, 129385m.
7. Saint plus for Windows NT, Bruker AXS, 1999.
8. Sheldrick, G. M. *SHELXTL NT Ver. 5.1*, Bruker AXS, 1998.
9. Sheldrick, G. M. *SHELXS-97*, Program for structure solution, University of Göttingen, Germany, 1997.
10. Sheldrick, G. M. *SHELXL-97*, Program for structure refinement, University of Göttingen, Germany, 1997.
11. Schouten, A.; Kanters, J. A.; Kroon, J.; Looten, P.; Duflot, P.; Mathlouthi, M. *Carbohydr. Res.* **1999**, *322*, 274–278.